Princeton Plasma Physics Laboratory

PPPL- 5159

USING ACOUSTIC DETECTORS TO MONITOR ITER ICH TRANSMISSION LINES ARC EVENTS

C. C. Kung, E. Fredd, N. Greenough, G. D'Amico,
A. Castano, C. Brunkhorst, J. Hosea, R. H. Goulding, M. McCarthy,
P. Pesavento, I. H. Campbell

July 2015

PPPL PRINCETON PLASMA PHYSICS LABORATORY

Prepared for the U.S. Department of Energy under Contract DE-AC02-09CH11466.

Princeton Plasma Physics Laboratory
Report Disclaimers

Full Legal Disclaimer

Trademark Disclaimer

PPPL Report Availability

Princeton Plasma Physics Laboratory:

http://www.pppl.gov/techreports.cfm

Office of Scientific and Technical Information (OSTI):

http://www.osti.gov/scitech/

Related Links:

U.S. Department of Energy

U.S. Department of Energy Office of Science

U.S. Department of Energy Office of Fusion Energy Sciences

USING ACOUSTIC DETECTORS TO MONITOR ITER ICH TRANSMISSION LINES ARC EVENTS

C. C. Kung, E. Fredd, N. Greenough, G. D'Amico, A. Castano, C. Brunkhorst, J. Hosea
Princeton Plasma Physics Laboratory
James Forrestal Campus, Princeton University
Princeton, NJ 08543-0451, USA
ckung@pppl.gov

R. H. Goulding, M. McCarthy, P. Pesavento, I. H. Campbell
Oak Ridge National Laboratory
Oak Ridge, TN 37831-6169, USA

***Abstract*—Severe and continuous arcs in transmission lines systems can be detrimental to the RF sources and the associated transmission lines. In order to prevent any damage to the whole system, arc detection and protective system shutdown are required for ITER ICH operations. In this case, it is desired to locate and replace the damaged transmission line sections caused by the arcs during routine maintenance; thus identifying the arc location during each occurrence will be needed to facilitate the maintenance work. There have been quite a few proposals for localizing the arcs positions in the past. However, there has been no major breakthrough in this research topic especially when the number of detectors is finite and limited. Because the ITER transmission lines are pressurized with dry air, each arc event will be accompanied with a shock wave propagating through the transmission lines. In this case, it is possible to determine the arc location by using two acoustic detectors in the transmission line under ideal conditions.**

Keywords—ITER ICH; transmission lines; arcs; locations; acoustic shock waves

I. INTRODUCTION

It is very common to have severe and continuous arcs in transmission lines systems during high power ion cyclotron heating (ICH) for magnetic fusion energy research operations. These arcs can be detrimental to the RF sources and the associated transmission lines. In order not to damage the whole system, arc detection and protective system shutdown are required for ITER ICH operations[1]. Even though the successful implementation of this requirement could prevent any possible major damage to the system and have almost no impact to the operations, it might be still desired to locate and replace the damaged sections during routine maintenance. Under this circumstance, it is required to identify the arc location during each occurrence.

There have been quite a few proposals for localizing the arcs positions in the past[2]. However, there has been no major breakthrough in this research topic especially when the number of detectors is finite and limited. Because the ITER transmission lines are pressurized with dry air, each arc event will be accompanied with a shock wave propagating through the transmission lines. As shown in Fig. 1, the shock wave propagation is confined to 1-dimensional flow in two directions with speed V and two acoustic detectors are separated with distance d. When there is an arc in the transmission line, detector 1 and 2 will record the shock wave with time stamps t1 and t2 respectively. In this case, it is possible to determine the arc location by solving two concurrent equations: d1+d2 = d and d2−d1 = V*(t2−t1). This leads to d1 = [d−V*(t2−t1)]/2 and d2 = [d+V*(t2−t1)]/2, and thus the arc location can be found.

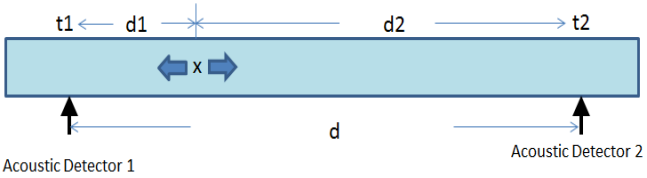

Fig. 1. Acoustic detector 1 and 2 are placed in two locations separated by distance d in the transmission line system. When arc occurs at x and the shock wave propagates at speed V in two directions and arrives at detector 1 and 2 with time stamps t1 and t2 respectively, the arc location in the transmission line is either d1 = [d−V*(t2−t1)]/2 or d2 = [d+V*(t2−t1)]/2.

In this study, we have first created an arc with a spot knocker in the laboratory to characterize the associated shock wave with different microphones. Since the shock wave energy is directly derived from the arc, different methods were used to estimate the energy in this artificial arc. Due to some difficulties to generate an arc in the transmission line, we mimicked the arc shock wave with a pulse generator and an audio amplifier to drive a high fidelity speaker. By comparing the energy levels between the artificial arc shock wave and the speaker acoustic wave, we were able to use the acoustic wave to simulate shock wave propagation under variable conditions in the transmission line system located at Oak Ridge National Laboratory (ORNL).

II. ARTIFICIAL ARC AND SHOCK WAVE GENERATION

The circuitry to generate the arc and the associated shock wave will be described in details. Because the shock wave energy is the key to this study, different methods were used to estimate the shock wave energy level.

A. Artificial Arc Generation

A spot knocker circuit was used to generate the arc. It consists of a 0 – 75 kV Hippotronics power supply, a small storage capacitor, and a discharge resistor. The maximum available energy from the system 2.5-nF capacitor is 14 J. The spark gap in the spot knocker was formed with two 5/8" diameter silver coated brass balls. A Pearson Electronics Pulse

*Work supported by U.S. DOE Contract No. DE-AC02-09CH11466

Current Transformer (Model 1025), whose conversion ratio is 12.5 mV/A with 50-Ω termination, in conjunction with a Tektronix TPS 2024 Digital Oscilloscope was used to monitor the arc current. In order not to overload the oscilloscope, a 20-dB attenuator and a 50-Ω terminator were connected to the oscilloscope input. Detailed description of this spot knocker circuit is shown in Fig. 2.

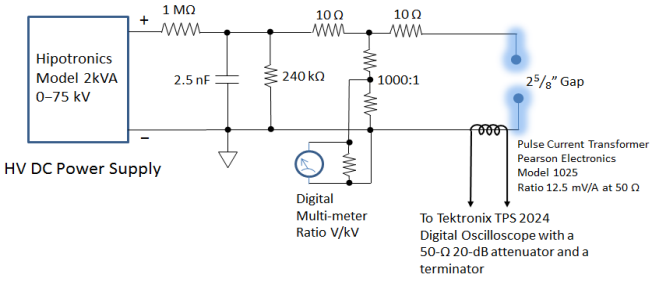

Fig. 2. Circuit diagram and test setup for the spot knocker; the spark gap consists of two 5/8" diameter silver coated brass balls.

When the spark gap size was set at 2.625", it arced sporadically at 53 kV. The corresponding field strength at this 2.625" gap is 7.95 kV/cm and the stored energy in the 2.5-nF capacitor is 3.5 J. In terms of 50-Ω transmission line, this gap size corresponds to 9.3"-diameter line. Note that the breakdown field strength in dry air at 1 atm under ideal conditions is 29 kV/cm between two parallel plates. This reduced field strength is mainly due to the moisture/humidity and the curvature of the balls.

B. Energy in the Artificial Arc

Based on Pearson Current Transformer in the presence of an arc, the main current waveform fluctuates between 800 A and 2.4 kA and lasts approximately 200 ns (Fig. 3). By using Ohm's law and average current flow (1.6 kA), the energy in the arc is (53 – 1.6*20) kV*1.6 kA*200 ns=6.72 J. However, the fast time scale on the oscilloscope indicates that an estimated factor of 25% should be included in the current waveform, this leads to 6.72*0.25=1.68 J. By using the same token, the energy dissipated in these two 10-Ω resistors is 0.25*(20*1.6) kV*1.6 kA*200 ns=2.56 J. Because of energy conservation, the total dissipated energy shall be less than 3.5 J. Since the HV DC Power Supply can provide up to 20 mA to recharge the 2.5-nF capacitor (132.5 μCoul at 53 kV), this capacitor will be ready for the next arc (breakdown) in less than 10 ms. Thus, the arcing energy in this setup is very possible between 1 and 2 J. However some further investigations will be needed to verify this estimation.

Note that slow oscilloscope time scale clearly reveals the ensemble of the current waveform is very close to Sinc function with the first null at 250 ns. This indicates that the acoustic waves derived from this shock wave will have a flat spectral distribution as high as 4 MHz. However, Pearson Current Transformer (Model 1025) frequency response is between 160 Hz and 4 MHz at 3-dB points. In this case, the acoustic waves spectral distribution can be very possible far beyond this 4-MHz limit. Because the time duration is very short (~200 ns), this 1−2 J of energy (5−10 MW for the corresponding power levels) will heat up the air column along the arcing path and a shock wave will be generated from this fast expanding air column. The observed intense blue color in the arc is due to the neutralization process of those singly ionized nitrogen atoms[3-4].

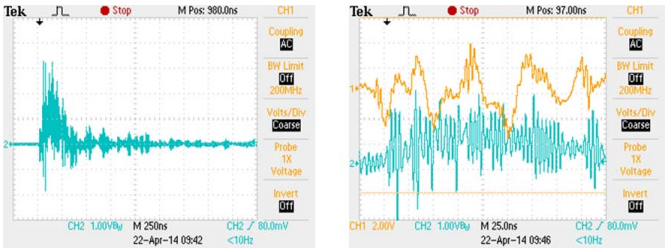

Fig. 3. Two current waveforms (Blue Traces) from the Pearson Current Transformer in different time scales; the fast time scale reveals the transformer bandwidth limit (~4 MHz).

C. Sound Level Meter Measurement

In order to detect the shock wave, Protek SL100 Sound Level Meter, which measures between 31.5 Hz and 8 kHz, is used to estimate the sound intensity. It was found that the meter was overloaded when the meter is less than 5 ft away from the spark gap. The measured values at 5 ft away are 110±2 dB, this corresponds to 0.1 W/m^2. Because this distance is much larger than the gap size (5' >> 2.625"), we can assume that the shock wave is a point source and the total power is well distributed on a spherical surface of 5' (1.5 m) radius. Thus the measured power in the shock wave is 0.1*4 π *1.5^2=2.8 W.

Note that there are two factors to determine the measured power for any power meter; they are the measured bandwidth and the integration time. The bandwidth ratio for this meter, which is from >4 MHz to 8 kHz, is between 500 and 1000. In order to measure down to 31.5 Hz for this meter, the integration time has to be longer than 32 ms. The ratio between the arc pulse width < 1 μs and this integration time ratio is greater than 30,000. Thus the estimated shock wave instantaneous power is between 40 and 80 MW. By using 200-ns in the current waveform, the corresponding energy level is 8−16 J and is much greater than the available energy (3.5 J). This is due to the long integration time of the sound level meter and the finite enclosed space, the sound level meter might register multiple reflections from the walls and the cabinets in the room.

D. Commercial Microphone Measurement

Because it is required to have an acoustic detector to mount on the side of the transmission line to detect the shock wave, a commercial available microphone might be the best candidate for this proof-of-concept project. As for most of mid-price microphones, they have an acoustic response in the range of 12−15 kHz corresponding to the mechanical resonance of the diaphragm that shapes the upper end of their treble response. Also flat tops are observed on those microphone oscilloscope traces. This type of signal limiter behavior might be due to overloading the microphone's FET amplifier at high sound pressure levels.

A CMI-5247TF-K microphone of CUI Inc., which has much smaller form factor, has been selected to detect the shock wave. The microphone appearance drawing with dimensions is

shown in Fig. 4(a). The recommended measurement circuit diagram is in Fig. 4(b) and the corresponding operating frequency is between 70 Hz and 20 kHz as indicated in Fig. 5. Based on its specifications, the minimum sensitivity of this microphone can be as low as -47 dB (V/Pa) with 60 dBA signal-to-noise ratio. Note that the base (0 dB) for acoustic (sound) pressure is 20 µPa and its corresponding sound intensity is equal to 1 pW/m^2. During the test, this microphone was placed 2 ft away from the spark gap in an open environment.

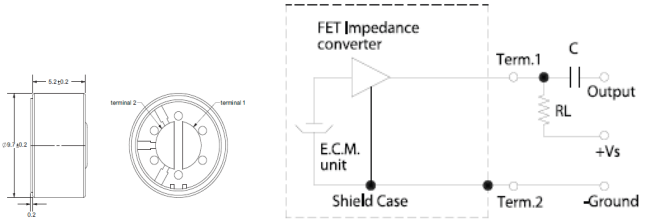

(a) (b)

Fig. 4. CMI-5247TF-K microphone of CUI Inc; (a) microphone dimensions in mm, the cross-section diameter is 9.7 mm (~3/8"). (b) recommended measurement circuit, where RL=680 Ω.

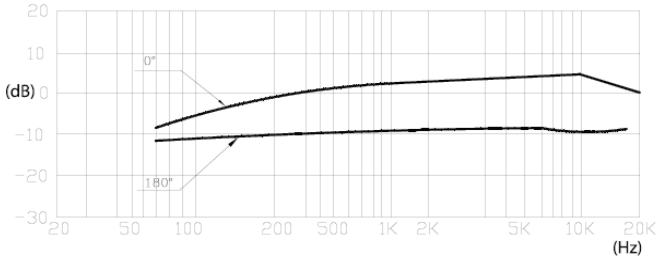

Fig. 5. Audio frequency response for CMI-5247TF-K microphone

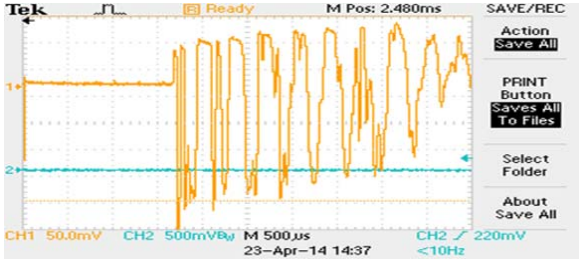

Fig. 6. Audio Waveform (Yellow Trace) obtained from CMI-5247TF-K of CUI Inc. at 2 ft away from the spark gap.

The oscilloscope trace is shown in Fig. 6. Since the arc current noise can easily propagate through the ground plane to trigger the oscilloscope (the pre-pulse on the trace), it shows that the microphone signals appear 1.7 ms later after the trigger. Note that the shock wave from the arc will strike whatever surface it encounters and this impacted surface will vibrate at its resonant frequency, which depends on its characteristics, to cause air pressure variations (pressure wave). This is the sound wave. It is a type of longitudinal wave and its propagation speed in air is $\sqrt{\Delta p/\Delta\rho}$, where Δp is the pressure change and Δρ is the air density change[5]. At 1 atm and 25℃, the sound speed is 346 m/s (approximate 1.1 ft/ms). Based on this 1.7 ms delay, it clearly suggests that the shock wave energy should be low enough and propagate at sound speed. Also, the trace shows that the shock wave forces the microphone diaphragm to move in one direction like compressing a spring and then its relaxation corresponding to the mechanical resonance appears in the first few cycles (fast rise/fall time and flat top). Due to the damping characteristic in the diaphragm and the transducer, rise/fall time and amplitude reduce accordingly in the later resonant cycles. The entire resonant phenomenon might last for few milliseconds.

III. Artificial Shock Wave and Acoustic Wave

In this section, it will be discussed how to mimic the arcing sound by using a waveform generator and an audio amplifier to drive an 8-Ω un-baffled speaker as well as how the acoustic wave propagates in a pipe.

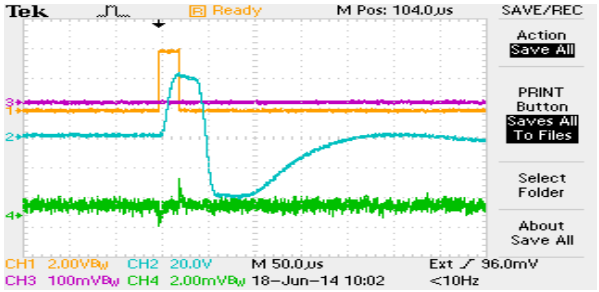

Fig. 7. Square pulse of 25-µs duration at the audio amplifier input (Yellow trace) and the corresponding audio amplifier output (Blue trace) to drive an 8-Ω 15 W speaker; the estimated pulse energy to this 8-Ω load is ~20mJ and the corresponding peak power is 200 W.

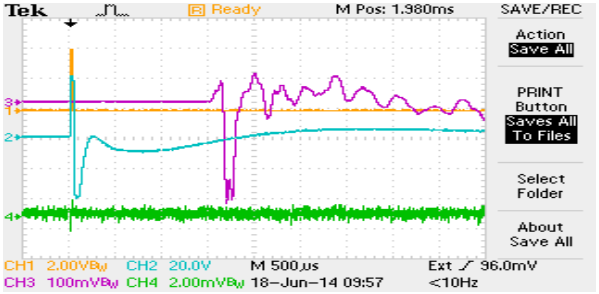

Fig. 8. Typical microphone (CMI-5247TF-K) output waveform (Violet trace) when it is driven by the 8-Ω 15 W speaker with the prescribed waveform (Blue trace)

A. *Artificial Shock Wave Generation*

Initially, we used different microphones to record the arc sounds into audio files and then intended to use a speaker to replay the sounds from those files. Thus, we can eliminate the danger of operating a high voltage power supply. However, due to finite audio bandwidth in the microphone and the speaker as well as first few unwanted resonant cycles with saturated amplitudes on the microphone waveform, it sounds very different from the original arc sounds by using our human ears. In other words, the performance limitations of the microphone and the speaker can easily distort the arc sounds and truncate the high frequencies portion of the shock wave. Since the shock wave is a fast impulse and the bandwidth limit in the microphone/speaker restricts the performance, it is possible to use the pulse generator to provide a square pulse of 25-µs duration as an impulse to the speaker. Because the pulse energy is too low to drive an 8-Ω un-baffled speaker, an audio

amplifier is used to increase the output pulse energy to ~20 mJ and the corresponding peak power is 200 W.

As shown in Fig. 7, the amplifier output pulse shape has 15-μs rise/fall time and ~30-μs pulse width at the half power point caused by the audio amplifier distortion. If we treated this ~30-μs audio amplifier pulse as a half cycle, the corresponding frequency would be 1/(2*30 μs)=16.7 kHz. In other words, this is the upper frequency limit that the audio amplifier can deliver under these conditions. Since this frequency is also the upper bound response for most of the microphones and some high frequency speakers (such as tweeters), that is why the sound perception with our ears and the signals in time and frequency domain are very similar to an arc shock wave with much less intensity.

Note that the microphone waveforms shown in Fig. 6 and Fig. 8 have the same resonant period with much less amplitude in Fig. 8. This clearly indicates that the same microphone preserves its own damping and resonant characteristics under different shock/acoustic wave energy levels. In other words, this acoustic wave generation and detection by using a pulse generator/speaker and a microphone can be a useful tool to simulate the shock wave propagation in a gas-filled pipe, tube, waveguide, or coaxial transmission line.

B. Sound Wave Propagation in a Pipe

As mentioned earlier, the sound wave is a type of pressure wave. It can be understood as small modulations in terms of pressure and density on the localized compressible fluid and its propagation speed in the compressible fluid is $\sqrt{\Delta p/\Delta \rho}$. Because p (pressure) is directly proportional to ρ (density), the sound wave speed will not change in any pressure levels. If this localized compressible fluid were moving at certain speed in laminar flow, the sound wave pitch (frequency) would be affected by the Doppler effect. The pitch might turn higher when the sound wave is propagating in the same direction of the moving fluid and the pitch might turn lower when the sound wave is propagating against the direction of the moving fluid. However, the sound wave pressure wave front might be fully distorted if the compressible fluid were in turbulent flow. In this case, sound wave properties might become extremely difficult to characterize at the detection point.

As for the sound wave propagating in a pipe with its diameter smaller than the sound wavelength (e.g. ~1 ft for 1 kHz sound wave), the sound wave propagation will be along the pipe (1-dimension flow). Because the sound pressure wave is confined along the pipe and is normal to the pipe cross-section, there is no $1/r^2$ propagation loss when the acoustic transducer (e.g. microphone) is at distance r apart. If the pipe wall is smooth enough and the friction loss (particles drag force on the pipe wall) is negligible, there should not be any measureable sound wave power loss at the transducer[6]. On the contrary, the sound wave might sustain some $1/r$ propagation loss if the pipe diameter is larger than the wavelength.

The test setup to monitor the sound wave propagation in a pipe is shown in Fig. 9. The CMI-5247TF-K microphone was placed at the end of a 6"-diameter 30" long pipe. Since the microphone effective reception area is only of ~3/8" diameter, it can only receive 0.4% of the sound wave energy in the pipe based on the geometrical factor. By using the waveforms shown in Fig. 7 to drive the speaker, the microphone response waveforms with different time scales are shown in Fig. 10.

Note that the rise/fall time of the audio amplifier output waveform is ~25 μs and the observed rise/fall time at the speaker output is ~50 μs and the waveforms at the end of the pipe is ~100 μs. This ~50-μs rise/fall time at the speaker output is due to the finite bandwidth in the microphone and the speaker. Because the pipe diameter is of 6", the sound wave greater than 2 kHz will also propagate radially in this pipe. Thus, the rise/fall time will be further reduced due to the path loss (possibly $1/r$ propagation loss in radial direction of the pipe) for those signals higher than 2 kHz frequencies. A cone shape collector might be needed for the microphone in order to preserve the pulse shape of ~50-μs rise/fall time.

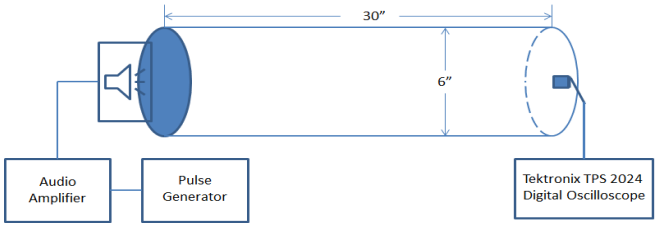

Fig. 9. The test setup to monitor the sound wave propagation in a pipe

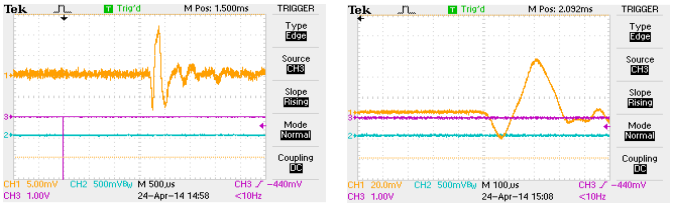

Fig. 10. Speaker-Microphone waveforms (yellow traces) derived from the output of a pulse generator/audio amplifier through a 30" long pipe of 6" diameter.

IV. Shock Wave in the Transmission Line

With the help of speaker-microphone pair to simplify the arc shock wave generation/detection, it is possible to perform the experiment on the ITER-like transmission line system. How to do the experiments will be discussed in this section.

A. Resonant Ring

According to the specifications, ITER ICH transmission line systems have to transmit up to 6 MW continuously. The corresponding voltage in a 50-Ω line will be ~25 kV. Resonant ring, which couples small amount of RF power into a high-Q resonant ring cavity structure, was developed in order to test the transmission line components without a 6-MW RF source. This resonant ring located at ORNL is capable of increasing the voltage/current to the desired levels inside the ring. Upon inserting the RF component in the correct location inside the ring, its performance can be verified against the ITER specifications. In order to prevent arcs inside the ring and remove excess heat, the ring is filled with 3-bar dry air and equipped with a blower capable of circulating the dry air up to 10 m/s per ITER specifications[7].

Because of those unique features of the resonant ring, it becomes the best candidate to test the shock wave propagation inside the ITER-like transmission line. In order to understand the shock/acoustic wave propagation, 4 microphones and a speaker were installed on the outer conductor wall of the resonant ring transmission line. As indicated in Fig. 11, angled view ports and straight sensor ports were the locations to place the microphones and the speaker was mounted at the gas tee flange on the opposite side. With properly developed adaptors, speaker and microphones were mounted in hermetic structures to withstand 3 bars of pressure. The 8-Ω 15 W speaker is shown in Fig. 12(a) and the CMI-5247TF-K microphone of CUI Inc. in a copper enclosure to reduce the EMI during an arc is shown in Fig. 12(b).

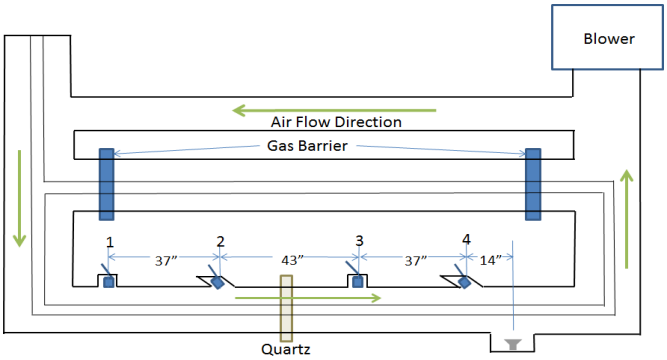

Fig. 11. Angled view ports and straight sensor ports are the locations to place the microphones and the speaker is mounted at the Gas tee flange on the opposite side.

(a) (b)

Fig. 12. (a) 8-Ω 15 W speaker driven with a square pulse into an audio amplifier to mimic the arcing sound; (b) CMI-5247TF-K Microphone of CUI Inc. in a copper enclosure to reduce the EMI during an arc.

B. Results with Low Blower Speed

The blower, which has 6 blades with 1:1 belt drive and is powered with 480 Vac, can provide full blowing power while its motor is rotating at 3500 RPM. During the operation, the motor power control can be set at 4 different levels. They are 25%, 50%, 75% and 100% of its full power.

Initially, the setup was tested at 1 bar with blower off. The results are shown in Fig. 13. The oscilloscope was externally triggered by the pulse generator and the triggered time was indicated by a downward arrow on the scope. Because microphone 4 is opposite to the speaker, the sound wave propagation has to include the transmission line diameter (13”) and thus the diagonal distance becomes 19” and the required propagation time is 1.4 ms. For microphone 3, which is 37” from 4, the time difference is 2.8 ms. By the same token, the time difference between microphone 2 and 3 would be 3.2 ms (43” apart) as well as between microphone 1 and 2 would be 2.8 ms (37” apart).

Then the blower was turned on at 25% of its full power and the pressure was still at 1 bar (Fig. 14(a)), then the pressure was increased to 3 bar (Fig. 14(b)). Fig. 14 clearly indicates that the gas pressure has no influence on the sound wave propagation speed. Because the speaker and microphones are mounted sideway on the transmission line, certain propagation loss will be encountered due to echoing inside the transmission line and zero air velocity on the transmission line wall. Thus, the signal strength on each microphone will suffer some degradation. That is why the signal becomes weaker when the microphone is farther away from the speaker. Also because of the quartz support, some further degradation appears at microphone 1 and 2. It can be observed that the air flow is laminar flow when the blower is at 25% of the full power and has no impact on the sound wave propagation.

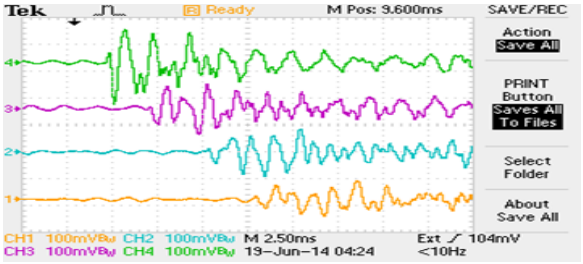

Fig. 13. The microphones signals while the transmission line was under 1 bar pressure with blower off; the oscilloscope was externally triggered by the pulse generator and the triggered time was indicated by a downward arrow on the scope.

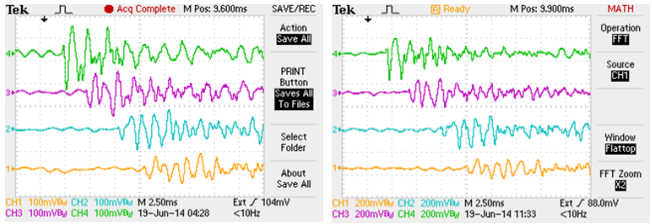

(a) (b)

Fig. 14. The microphones signals while the blower was at 25% of the full power; (a) the transmission line was under 1 bar pressure, (b) the transmission line was under 3 bar pressure.

C. Results with High Blower Speed

The microphones signals, while the transmission line was under 3 bar pressure and the blower was at 75% and 100% of the full power, are shown in Fig. 15(a) and (b) respectively. It clearly indicates that the air flow becomes turbulent flow and the artificial arc signals from the speaker are difficult to differentiate.

It is possible to believe that the blower speed is directly proportional to the power level. Based on 6 blades, 1:1 belt drive, and 3500 RPM at 100% full power, the corresponding fundamental fluctuations of air flow in the transmission line are 87.5 Hz at 25%, 175 Hz at 50%, 262.5 Hz at 75%, 350 Hz at 100%, and their higher harmonics as well as the sub-harmonics directly proportional to the rotor speed. By using FFT on one of the microphones signals, ~180 Hz and its harmonics appears

at 75% of the full blower power (Fig. 16(a)) and ~750 Hz appears at 100% of the full blower power (Fig. 16(b)).

The power spectrum from the microphones signals, while the transmission line was under 3 bar pressure with blower off, is shown in Fig. 17. It clearly shows that it has much lower noise signal floor below 1 kHz when compared to the floor shown in Fig. 16. Thus, the possible blower contributions from the rotor and the blades in power spectrum would be all below 1 kHz at any power level. In this case, it is possible to use simple RC high pass filter at the microphone output to remove the blower noise.

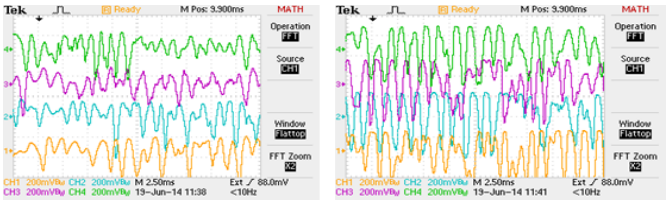

(a) (b)

Fig. 15. The microphones signals while the transmission line was under 3 bar pressure (a) the blower was at 75% of the full power, (b) the blower was at 100% of the full power.

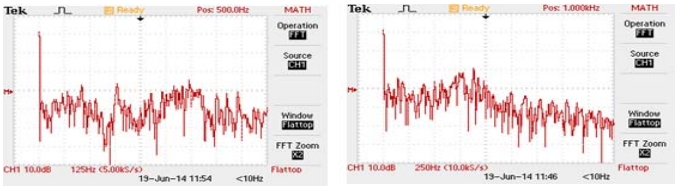

(a) (b)

Fig. 16. The power spectrum from the microphones signals while the transmission line was under 3 bar pressure (a) the blower was at 75% of the full power, (b) the blower was at 100% of the full power.

Fig. 17. The power spectrum from the microphones signals while the transmission line was under 3 bar pressure with blower off.

Based on the power spectrum data and the wide spectral distribution of the shock wave in an arc, ultrasonic detector with a proper high pass filter to remove the blower noise can be considered as a superior candidate for acoustic arc detection in the future. Because the gas flow speed is less than 10 m/s when the blower is at 100% full power, this is much less than the sound speed (346 m/s) at 25℃ and thus the Doppler effect can be negligible in terms of detecting the shock/acoustic wave signals.

CONCLUSIONS

Arcs with possible 1−2 J of energy are generated with a high voltage power supply and a spot knocker. Based on the Pearson pulse current transformer, the arc duration is ~200 ns and the associated pulse power is 5 −10 MW. Because of finite bandwidth of the pulse current transformer (~4 MHz), the estimated shock wave spectrum in each arc should be >4 MHz. Finite bandwidth of the microphone and the speaker makes the replay arc sounds very close to the sound of a deformed 25-μs pulse, which is generated by a pulse generator and an audio amplifier. Unfortunately, the available energy in this pulse is ~20 mJ. With the knowledge of man-made shock wave energy level and audio amplifier limit, the acoustic arc localization feasibility experiment can be performed with a speaker driven by a pulse generator and an audio amplifier. Time domain signals from each microphones under 1-bar and 3-bar pressure clearly indicate that the sound wave propagation speed is independent of the gas pressure. Because of the blower configuration and motor speed, the spectral signature from the FFT signals for the blower at any speed is below 1 kHz. The experimental results show that there is almost no impact to the acoustic signals while the blower is operating below 25% of the full power. Only when the blower speed is above 75% of the full power, the microphone signals are all inundated with blower noise. Note that RF arcs and dc arcs are very different. Depending on the transmission line/antenna surface conditions, the RF arc only occurs at either the positive peak voltage or the negative peak voltage. For example, 50 MHz RF signals at 6 MW have only 60 mJ in a half cycle. Since the sound wave intensity is directly proportional to the shock wave energy, some further investigations will be needed to determine the possible energy level of an RF arc in the transmission line.

ACKNOWLEDGMENT

This work is supported by US DOE Contract No. DE-AC02-09CH11466. All US activities are managed by the US ITER Project Office, hosted by Oak Ridge National Laboratory with partner labs Princeton Plasma Physics Laboratory and Savannah River National Laboratory. The project is being accomplished through a collaboration of DOE Laboratories, universities and industry.

REFERENCES

[1] G. Bosia, “Automatic control of the ITER ion cyclotron system”, Fusion Eng. Des., 82 (2007), pp. 662-665.

[2] R/ D’inca, “Arc detection for the ICRF system on ITER”, AIP Conf. Proc. 1406, 5 (2011).

[3] Rakov and M. A. Uman, “Lightning : physics and effects”, Chapter 11 and 12, Cambridge University Press, 2003.J. Clerk Maxwell, A Treatise on Electricity and Magnetism, 3rd ed., vol. 2. Oxford: Clarendon, 1892, pp.68–73.

[4] Brian Lane Maas, “Arc Current, Voltage, and Resistance in a High Energy, Gas-Filled Spark Gap”, master thesis, May 1985. K. Elissa, “Title of paper if known,” unpublished.

[5] D. Halliday, R. Resnick, and J. Walker, “Fundamentals of Physics”, 9th edition, Chapter 17, John Wiley & Sons, Inc., 2011.

[6] F. Jacobsen and P. M. Juhl, “Fundamentals of General Linear Acoustics”, John Wiley & Sons, Inc., 2013.

[7] R. H. Goulding, et al, “Status of transmission line and matching network design and testing for the ITER ion cyclotron heating and current drive system”, AIP Conf. Proc. 1580, 370 (2014).

PPPL PRINCETON PLASMA PHYSICS LABORATORY

Princeton Plasma Physics Laboratory
Office of Reports and Publications

Managed by
Princeton University

under contract with the
U.S. Department of Energy
(DE-AC02-09CH11466)

P.O. Box 451, Princeton, NJ 08543
Phone: 609-243-2245
Fax: 609-243-2751

E-mail: publications@pppl.gov

Website: http://www.pppl.gov